



## **PRACTICAL APPLICATION OF TRANSVERSE LOAD REDISTRIBUTION IN REINFORCED CONCRETE SOLID SLAB BRIDGES**

Eva O.L. Lantsoght  
Universidad San Francisco de Quito, Quito, Ecuador  
Delft University of Technology, Delft, The Netherlands

Cor van der Veen  
Delft University of Technology, Delft, The Netherlands

Ane de Boer  
Ministry of Infrastructure and the Environment – Rijkswaterstaat, Utrecht, The Netherlands

### **ABSTRACT**

For an initial design or assessment of a reinforced concrete solid slab bridge, spreadsheet-based or hand calculations are typically used. The shear stress is compared to the shear capacity as prescribed by the code. The distributed loads result in a uniform shear stress at the support. Concentrated loads are less straightforward to take into account. It is known that transverse load redistribution occurs in slabs. To explore the topic of transverse load redistribution, experiments on elements subjected to a concentrated load close to the support were carried out. These elements had an increasing width, starting at 0.5 m and increasing with steps of 0.5 m up to 2.5 m, so that the effect of transverse load redistribution could be studied. The threshold effective width resulting from the experiments was then compared to load spreading methods, in order to give recommendations for the practical use with concentrated loads. It was found that the load spreading method as used in French practice is to be preferred. As compared to load spreading methods that were used previously, the French load spreading method results in smaller shear stresses at the support. This result allows for more economic designs and provides a better assessment tool.

### **1. ASSESSMENT PRACTICE**

#### **1.1 Situation in the Netherlands**

In the Netherlands, the topic of assessment of existing bridges has gained a lot of importance over the past years. The reason why assessment has become one of the main sources of research and projects, is related to the implementation of the Eurocodes combined with ageing of the Dutch bridge stock. The majority of the existing reinforced concrete bridges in the Netherlands were built in the decades following the Second World War, with a peak of construction in the late 1960s. Of the current bridge stock, 60% of the structures were built before 1975. Since then, the traffic loads and volumes have increased significantly. As a result, the live loads in EN 1991-2:2003 (CEN 2003) are heavier than in the previously used national codes. At the same time, there is a development towards expressions for the shear capacity in the Eurocodes that allow for smaller shear capacities than previously used national codes. The shear capacity given in EN 1992-1-1:2005 (CEN 2005) results in smaller shear capacities than when using the Dutch Code NEN 6720:1995 (Code Committee 351001 1995). Especially for deep sections with low amounts of longitudinal reinforcement, the Eurocode provisions allow for a significantly lower shear capacity.

A large number of the existing bridges in The Netherlands are reinforced concrete solid slab bridges. The majority of these bridges have 3 to 4 spans and a constant slab depth. The average main span is 13.5 m, the average end span is 10.1 m and the average total slab width equals 13.2 m. In a first round of assessments, it was found that 600 of

these reinforced concrete slab bridges required a more detailed study of their shear capacity, as they were designed in such a way that they could be shear-critical according to the current codes. Upon inspection, however, these bridges typically did not show signs of distress (Lantsoght et al. 2012a; Walraven 2010). This indicates that slab bridges possess additional sources of bearing capacity that are not taken into account in the concrete design codes. In slabs, one of the major sources of additional capacity is the slab's ability for transverse load redistribution.

## 1.2 Level of Approach Assessment

The new *fib* Model Code 2010 (*fib* 2012) for structural concrete defines different Levels of Approximation for a calculation. Amongst others, the shear and punching shear capacity can be determined based on the increasing levels of approximation. The first Level of Approximation uses a simplified formula, and takes little time and computational effort. Higher levels of approximation require more time and computational effort, but result in a better approximation and a less conservative estimate of the capacity, as sketched in Figure 1.

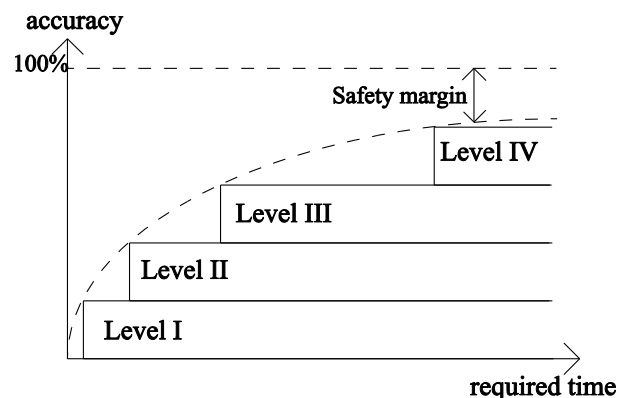


Figure 1: Illustration of the increasing Levels of Approximation, as defined by *fib* Model Code 2010 (*fib* 2012).

A similar approach can be used for assessment. The first Level of Approximation is a coarser assessment method, typically a hand calculation or a spreadsheet. If more accurate results are needed, a higher Level of Approximation is necessary – for example a numerical model.

In the Netherlands, the philosophy of Levels of Approximation is followed for the assessment practice of existing slab bridges. The first Level of Approximation is a spreadsheet-based method, called the Quick Scan method (Vergoossen et al. 2013). The result of the Quick Scan is a Unity Check: the ratio of the design shear stress over the design shear capacity (Lantsoght et al. 2013a). This approach was originally developed in the mid-2000s by engineering offices in the Netherlands, and is similar to a hand calculation. Over the next years, the method was improved by fine-tuning the method through the results of slab shear experiments (Lantsoght et al. 2013b). The beneficial effect of transverse load redistribution was taken into account by defining the effective width in shear that can be used in the Quick Scan method (Lantsoght et al. 2014). The practical method to take into account the transverse load redistribution capacity of slabs is the topic of the current paper. The Quick Scan is a fast, simple and conservative tool that can use the database of the existing slab bridges as its input, and that gives all Unity Checks of a selected number of cross-sections of these bridges as its output. As such, it helps to prioritize the assessment efforts and to identify which bridges need further study.

When the value of the Unity Check of a structure's cross-section is larger than 1, a Level II method of Approximation needs to be used. As shown in Figure 1, a Level II method is more time-consuming but the result is a closer estimate of the real bearing capacity of the structure. For the existing slab bridges, the second Level of Approximation is the use of a linear finite element model to determine the design shear stress at the support. Higher levels of approximation include the use of non-linear finite element models and probabilistic analyses.

## 1.3 First Level of Approach method

This paper focuses on assessment according to the First Level of Approach. For an initial design or assessment of a reinforced concrete solid slab bridge, spreadsheet-based methods or hand calculations are typically used, which we

can consider a first Level of Approach. The recommendations for load spreading that are studied in the current paper are results from studying the improvement of the first Level of Approach for assessment. However, since these recommendations are the direct result of a comparison between proposed methods and experiments, they are universally valid and can be used for design as well.

When the Quick Scan method is used, the result is the Unity Check, which was defined earlier as the ratio of the design shear stress over the design shear capacity. The design shear stress results from the composite dead load (self-weight of the slab and superimposed load as a result of the applied wearing surface) and the live loads, which are a combination of distributed lane loads and concentrated wheel loads. The Unity Check is carried out at the face of the support. The distributed loads result in a uniform shear stress, while the concentrated loads will cause a peak in the shear stress distribution. The loads are placed so that the largest shear stress is found at the edge of the slab, as this location was earlier indicated to be the governing section for slab bridges (Cope 1985). The denominator of the Unity Check, the design shear capacity, is determined according to EN 1992-1-1:2005. This paper focuses on the distribution width of the concentrated loads.

## 2. LIVE LOADS

The concentrated loads that are studied result from the live loads. To determine the shear stress at the support, the live loads from EN 1991-2:2003 (CEN 2003) Load Model 1 are used for assessment. This Load Model (Figure 2) combines design trucks with a design lane load that is heavier in the first, slow lane. A design truck with 2 axles of each 2 tires, with a tire contact of  $400\text{mm} \times 400\text{mm}$ , is used. The design truck has an axle load of  $\alpha_{Q1} \times 300\text{kN}$  in the first lane,  $\alpha_{Q2} \times 200\text{kN}$  in the second lane and  $\alpha_{Q3} \times 100\text{kN}$  in the third lane. The values of  $\alpha_{Qi} = 1$  for the Netherlands. The lane load is applied over the full notional lane width (3m) and equals  $\alpha_{qi} \times 9\text{kN/m}^2$  for the first lane and  $\alpha_{qi} \times 2.5\text{kN/m}^2$  for all other lanes. In the Dutch National Annex, for bridges with 3 or more notional lanes, the value of  $\alpha_{q1}$  equals  $\alpha_{q1} = 1.15$  and for  $i > 1$  the value can be taken as  $\alpha_{qi} = 1.4$ .

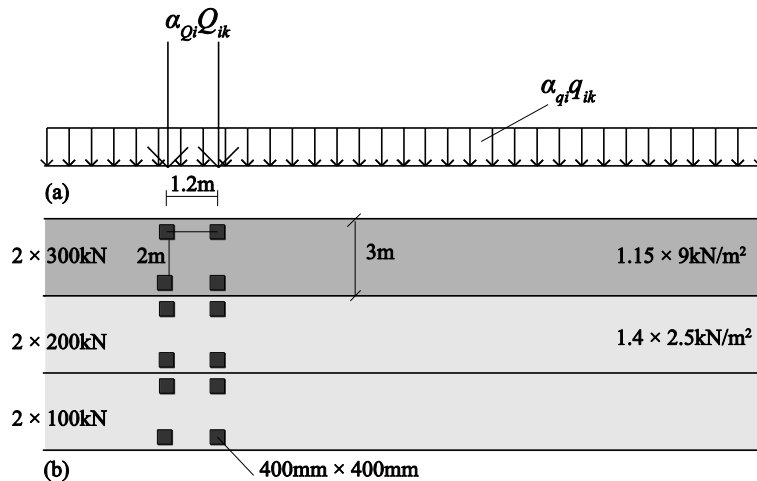


Figure 2: EN1991-2:2003 Load Model 1 (a) side view; (b) top view.

## 3. TRANSVERSE LOAD REDISTRIBUTION

### 3.1 Principle of transverse load redistribution

When concentrated wheel loads are applied to slabs, a peak stress will result in the shear stress distribution at the support. As such, not the full slab width is exposed to the same shear stress. By the same, not only the part of the support that has the same width as the concentrated load will be carrying the concentrated load. The concentrated load will be redistributed over a certain area around the load. This phenomenon is called transverse load redistribution, and it occurs for the case of concentrated loads on wide beams and slabs.

### 3.2 Load spreading methods

To quantify the amount of transverse load redistribution that occurs in slabs, load spreading methods are used in practice. A width at the support, which is larger than the width of the concentrated load, needs to be defined over which the load needs to be carried. In slabs and wide beams subjected to a concentrated load, the width at the support that carries the shear loading needs to be estimated; this width is the effective width in shear  $b_{eff}$ . Theoretically, the effective width  $b_{eff}$  is determined so that the total shear stress over the support equals the maximum shear stress over the effective width (Goldbeck 1917).

For calculations, the determination of this width depends on local practice: either a fixed width (for example, 1 m) is used or a horizontal load spreading method is used. Different load spreading methods are used in practice: from the center of the load to the face of the support under an angle of  $45^\circ$  as used in Dutch practice, resulting in the effective width  $b_{eff1}$  (Fig. 3a), from the far side of the load to the face of the support under  $45^\circ$  as used in French practice (Coin and Thonier 2007) (Fig. 3b) or with an angle depending on the type of support and to a certain distance away from the support as prescribed by the Model Code 2010 (fib 2012) (Fig. 3c). In Figure 3, the following symbols are used:

- $a$  is the center-to-center distance between the load and the support,
- $a_v$  is the face-to-face distance between the load and the support, and
- $d_l$  is the effective depth to the longitudinal reinforcement.

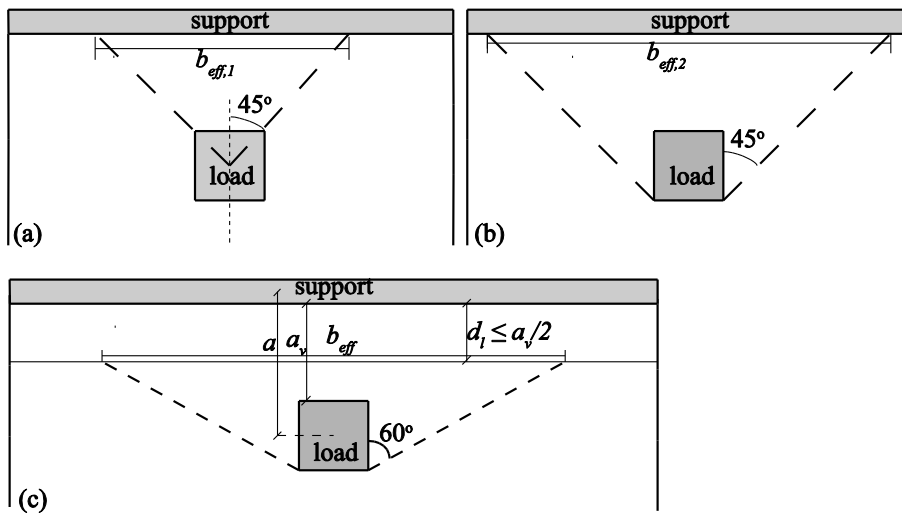


Figure 3: Top view of slab showing determination of effective width (a) assuming  $45^\circ$  horizontal load spreading from the center of the load:  $b_{eff1}$ ; (b) assuming  $45^\circ$  horizontal load spreading from the far corners of the load:  $b_{eff2}$ ; (c) load spreading as recommended by *fib* Model Code 2010 for loads near to simple supports.

### 3.3 Slabs versus beam from the literature

A series of experiments in which the specimen width is increased, with as purpose studying the influence of transverse load redistribution, has –to the authors’ knowledge- not been carried out in the past. However, in some series of experiments, specimens with increasing widths were studied, and these results can be used to learn more about the influence of the width on the resulting effective width.

Previous research (Regan and Rezaei-Jorabi 1988) showed increasing maximum shear capacities for slabs with a concentrated load placed at such a location that  $a / d_l = 5.42$  (with  $a$  the center-to-center distance between the load and the support and  $d_l$  the effective depth to the longitudinal reinforcement) for increasing widths (0.4 m to 1.2 m) up to a certain value (1 m), after which the maximum shear capacity remained around the same value. In other experiments (Reißen and Hegger 2013), however, a threshold value for the width resulting in a constant shear capacity for increasing widths, was not observed for a concentrated load placed at  $a / d_l = 4.17$  as the width increased (0.5 m to 3.5 m).

## 4. EXPERIMENTS ON SLAB STRIPS

### 4.1 Test setup

To study the effect of transverse load redistribution in reinforced concrete elements, a series of specimens with widths increasing from 0.5 m to 2.5 m were tested. The specimens are named based on their width: the BS-series of specimens are 0.5 m wide, the BM-series 1.0 m wide, the BL-series 1.5 m wide, the BX-series 2.0 m wide and the S-series 2.5 m wide. The tested elements all had a length of 5 m, with a span between supports of 3.6 m and a depth of 0.3 m. The slabs are a 1:2 scale representation of typical solid slab bridges from The Netherlands. Since these experiments are not full-scale, the size effect (Bažant and Kim, 1984) could play a role in members with a larger depth. However, no experiments on slabs under concentrated loads close to supports with depths larger than 300 mm are available for comparison and to study the influence of the size effect.

A top view of the test setup for the reinforced concrete elements is given in Figure 4. The line supports (sup 1 and sup 2 in Fig. 4) consist of a steel beam (HEM 300) of 300 mm wide, a layer of plywood and a layer of felt of 100 mm wide (Prochazkova and Lantsoght 2011), so that the support width equals  $b_{sup} = 100$  mm.

Experiments were carried out close to the simple support (sup 1, SS in Fig. 4) and close to the continuous support (sup 2, CS in Fig. 4), where the rotation is partially restrained by vertical prestressing bars that are fixed to the strong floor of the laboratory. Load cells were used to measure the force in the prestressing bars during the experiment. For the specimens of 0.5 m wide, only 1 prestressing bar was used, and for the specimens of 1.0 m wide, 2 prestressing bars were used. All wider elements were tested with 3 prestressing bars as shown in Figure 4.

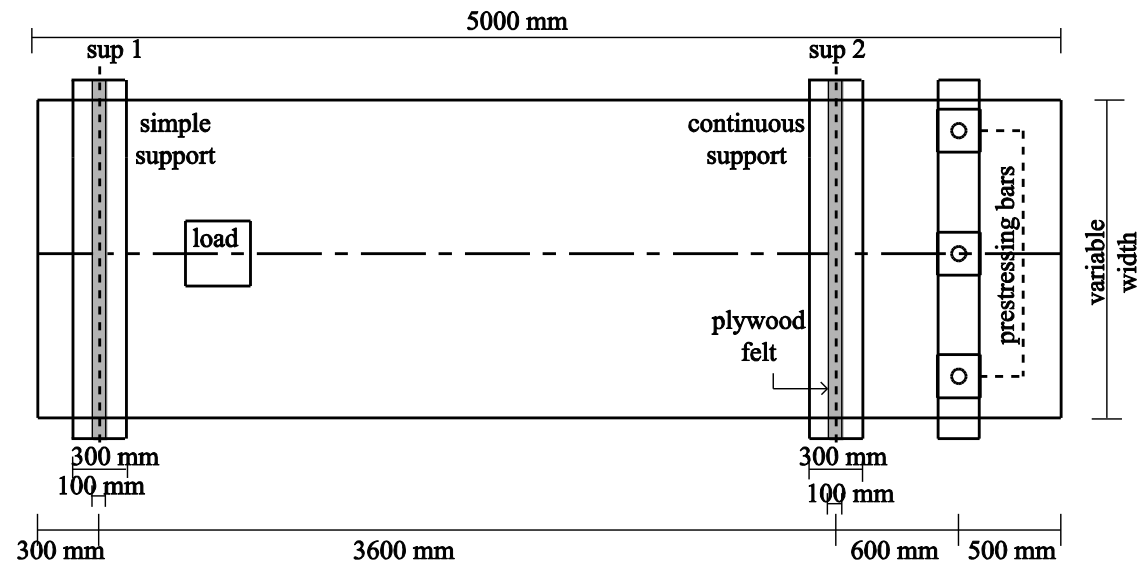


Figure 4: Sketch of test setup, top view.

The concentrated load was applied in a displacement-controlled way through a hydraulic jack onto a steel loading plate of 200 mm × 200 mm or 300 mm × 300 mm. The loading plate of 200 mm × 200 mm is a 1:2 scale representation of the 400 mm × 400 mm contact surface for each wheel of the axle load used in the live load model (Load Model 1) of EN 1991-2:2002 (CEN 2003), as shown in Figure 2. A full description of the materials and instrumentation, and the experimental observations are given in the full test report (Lantsoght 2011).

### 4.2 Specimens

The experimental program consisted of three reinforced concrete elements (BS-series) of 5.0 m × 0.5 m × 0.3 m, three elements (BM-series) of 5.0 m × 1.0 m × 0.3 m, three elements (BL-series) of 5.0 m × 1.5 m × 0.3 m and three elements (BX-series) of 5.0 m × 2.0 m × 0.3 m. The results of slabs S8 and S9 of 5 m × 2.5 m × 0.3 from a previous series of experiments (Lantsoght et al. 2013c) were used to complete the series of specimens with increasing widths.

An overview of the properties of these specimens is given in Table 1. In Table 1, the following properties are given:

$b$	is the specimen width
$f_{c,meas}$	is the measured cube compressive strength of the concrete
$f_{ct,meas}$	is the measured splitting tensile strength of the concrete
$\rho_l$ and $\rho_t$	are the reinforcement ratios of the longitudinal and transverse reinforcement respectively
$a$	is the center-to-center distance between the load and the support
$d_l$	is the effective depth to the longitudinal reinforcement
$z_{load}$	is the size of the side of the square loading plate, and
“age”	is the age of the specimen at which the first experiment was carried out, and at which the compressive and tensile properties of the concrete were determined.

All specimens were reinforced with deformed bars of steel S500. The deformed bars with a diameter of 20 mm had a yield stress of  $f_{ym} = 542$  MPa and an ultimate tensile strength of  $f_{um} = 658$  MP and the bars with a diameter of 10 mm had  $f_{ym} = 537$  MPa and  $f_{um} = 628$  MPa. A concrete cover of 25 mm to the reinforcement was applied. The effective depth to the longitudinal reinforcement  $d_l$  was 265 mm and the effective depth to the transverse reinforcement  $d_t$  was 250 mm. The reinforcement layout of the BS specimens is shown in Figure 5. For wider elements, the number of bars was increased to maintain the same reinforcement percentage for the longitudinal reinforcement of  $\rho_l = 0.948\%$ . For comparison to the previously tested slab specimens of 2.5 m, the percentage of transverse flexural reinforcement was kept at  $\rho_t = 0.258\%$ . High strength concrete of class C53/65 from EN 1992-1-1:2005 §3.1.2 (3) Table 3.1 (CEN 2005) was used with a target cylinder strength  $f_{c,cyl}$  of 61 MPa. Glacial river aggregates with a maximum aggregate size of 16 mm were used.

Table 1: Properties of specimens BS1 – BX3, plus S8 – S9 for comparison.

Specimen nr.	$b$ (m)	$f_{c,meas}$ (MPa)	$f_{ct,meas}$ (MPa)	$\rho_l$ (%)	$\rho_t$ (%)	$a$ (mm)	$a/d_l$	$z_{load}$ (mm)	age (days)
BS1	0.5	81.5	6.1	0.948	0.258	600	2.26	300	55
BM1	1.0	81.5	6.1	0.948	0.258	600	2.26	300	62
BL1	1.5	81.5	6.1	0.948	0.258	600	2.26	300	189
BS2	0.5	88.6	5.9	0.948	0.258	400	1.51	200	188
BM2	1.0	88.6	5.9	0.948	0.258	400	1.51	200	188
BL2	1.5	94.8	5.9	0.948	0.258	400	1.51	200	180
BS3	0.5	91.0	6.2	0.948	0.258	600	2.26	300	182
BM3	1.0	91.0	6.2	0.948	0.258	600	2.26	300	182
BL3	1.5	81.4	6.2	0.948	0.258	600	2.26	300	171
BX1	2.0	81.4	6.0	0.948	0.258	600	2.26	300	47
BX2	2.0	70.4	5.8	0.948	0.258	400	1.51	200	39
BX3	2.0	78.8	6.0	0.948	0.258	600	2.26	200	40
S8	2.5	77.0	6.0	0.996	0.258	600	2.26	300	48
S9	2.5	81.7	5.8	0.996	0.258	400	1.51	200	77

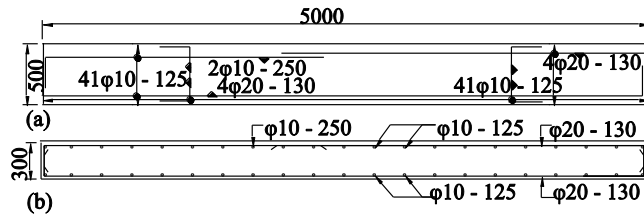


Figure 5: Reinforcement layout for test specimens: (a) top view of BS1; (b) cross-section of BS1; distances and diameters in [mm].

### 4.3 Results

On every specimen, one experiment was carried out at the simple support (SS in Fig. 4) and one at the continuous support (CS in Fig. 4). The results are reported in Table 2. In Table 2, the following symbols are used to report the results:

- $a$  is the center-to-center distance between the load and the support  
SS/CS is used for testing at the simple support (SS) or continuous support (CS)  
 $P_{exp}$  is the concentrated load at failure  
Mode is the failure mode, as shown in Figure 6  
 $F_{pres}$  is the sum of the forces in the prestressing bars, creating a moment over the continuous support  
 $V_{exp}$  is the shear force at the support due to the concentrated load, the force in the prestressing bars and the self-weight of the specimen  
 $V_{add}$  is the shear force due to the force in the prestressing bars and the self-weight of the specimen  
 $V_{conc}$  is the shear force due to the concentrated load only.  
As shown in Figure 6, the following failure modes are observed:
1. failure as a beam in shear with a noticeable shear crack at the side (B, Fig. 6a); or
  2. failure as a wide beam in shear with cracks at an angle of the span direction, resulting in inclined cracks on the bottom (WB, Fig. 6b);
  3. development of a partial punching surface on the bottom face (P, Fig. 6c).

Table 2: Experimental results for the tested specimens

Test	$a$ (m)	SS/CS	$P_{exp}$ (kN)	Mode	$F_{pres}$ (kN)	$V_{exp}$ (kN)	$V_{add}$ (kN)	$V_{conc}$ (kN)
BS1T1	0,60	SS	290	B	37	242	0	242
BS1T2	0,60	CS	623	B	212	562	43	519
BS2T1	0,40	SS	633	B	100	552	-11	563
BS2T2	0,40	CS	976	B	267	919	52	868
BS3T1	0,60	SS	356	B	57	293	-3	297
BS3T2	0,60	CS	449	B	107	399	25	374
BM1T1	0,60	CS	923	WB + B	160	811	41	769
BM1T2	0,60	SS	720	WB + B	127	591	-9	600
BM2T1	0,40	SS	1212	WB + B	167	1062	-15	1077
BM2T2	0,40	CS	1458	WB + B	262	1354	58	1296
BM3T1	0,60	SS	735	WB + B	110	607	-6	613
BM3T2	0,60	CS	895	WB + B	183	791	45	746
BL1T1	0,60	SS	1034	WB + B	215	844	-17	862
BL1T2	0,60	CS	1252	WB + B	320	1119	75	1043
BL2T1	0,40	SS	1494	WB + B	212	1311	-17	1328
BL2T2	0,40	CS	1708	WB + B	277	1586	68	1518
BL3T1	0,60	SS	1114	WB + B	242	907	-22	928
BL3T2	0,60	CS	1153	WB + B	312	1035	74	961
BX1T1	0,60	SS	1331	WB + P	325	1080	-30	1109
BX1T2	0,60	CS	1596	WB + B + P	335	1415	85	1330
BX2T1	0,40	SS	1429	WB + B + P	217	1259	-11	1270
BX2T2	0,40	CS	1434	WB + P	167	1332	57	1275
BX3T1	0,60	SS	1141	WB + P	245	935	-16	951
BX3T2	0,60	CS	1193	WB + B	210	1059	64	994
S8T1	0,60	SS	1481	WB + B	233	1226	-8	1234
S8T2	0,60	CS	1356	WB + B	278	1213	83	1130
S9T1	0,4	SS	1523	WB + P	175	1355	2	1354
S9T4	0,4	CS	1842	WB + P	255	1717	79	1637

## 5. COMPARISON BETWEEN LOAD SPREADING METHOD AND EXPERIMENTS

### 5.1 Measured threshold effective width

To define the threshold effective width for the shear capacity, the results of S8 and S9 (2.5 m) (Lantsoght et al. 2012b) are compared to the results of the current series of specimens (BS1 of 0.5 m to BX3 of 2 m), all of which are made with high strength concrete, Table 1. The results are displayed by showing the shear capacity as a function of

the member width in Figure 7. In Figure 7, the boundary line between “beams” and “slabs” at  $5h$  (with  $h$  the depth of the specimen) from EN 1992-1-1:2005 (CEN 2005) is also given. Additionally, the trendlines through datapoints at widths smaller than the threshold value are shown together with the lines of averaged constant shear capacities. The intersection of these lines determines the measured threshold for the considered series, defined by a set of constant parameters. These results show that the concept of using an effective width for wide members is indeed valid as the shear capacity does not increase linearly for larger widths. The results for the estimated threshold effective width based on the experimental results are given in Table 3 and compared to the calculated widths based on the load spreading methods from Figure 2. In Table 3, the following widths are defined:

- $b_{meas}$  is the threshold effective width based on the experiments
- $b_{eff1}$  is the effective width based on the Dutch load spreading method as shown in Figure 2a
- $b_{eff2}$  is the effective width based on the French load spreading method as shown in Figure 2b
- $b_{MC}$  is the effective width based on the *fib* Model Code 2010 (fib 2012) as shown in Figure 2c.

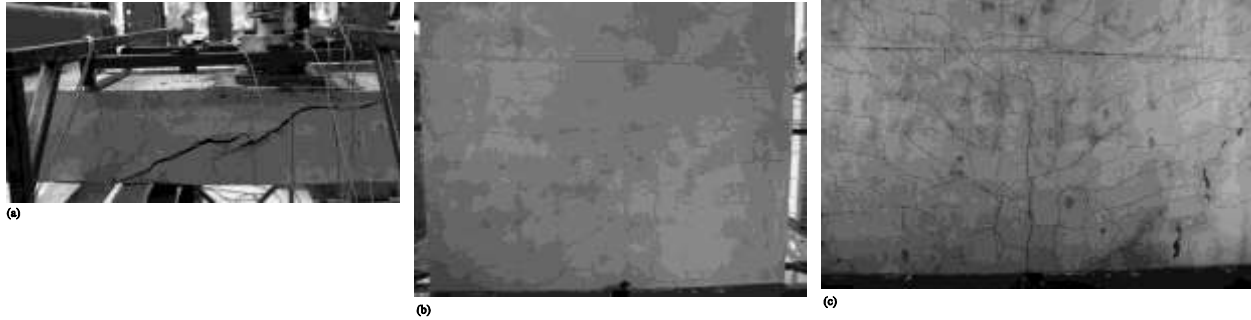


Figure 6: Observed failure modes: (a) B: shear crack at the side face (BS1T2); (b) WB crack pattern: inclined cracks on the bottom face (BL3T1); (c) P: partial punching at the bottom face (S9T1).

Table 3: Effective width as calculated from the experimental results, compared to the effective width based on the different load spreading methods.

No	Series	$b_{meas}$ (m)	$b_{eff1}$ (m)	$b_{eff2}$ (m)	$b_{MC}$ (m)
1	300 mm × 300 mm, SS, $a/d_l = 2.26$	2.0	1.1	1.7	1.0
2	300 mm × 300 mm, CS, $a/d_l = 2.26$	1.8	1.1	1.7	1.0
3	200 mm × 200 mm, SS, $a/d_l = 1.51$	1.3	0.7	1.1	0.6
4	200 mm × 200 mm, CS, $a/d_l = 1.51$	0.9	0.7	1.1	0.6
5	200 mm × 200 mm, SS, $a/d_l = 2.26$	1.5	1.1	1.5	1.0
6	200 mm × 200 mm, CS, $a/d_l = 2.26$	1.3	1.1	1.5	1.0

## 5.2 Influence of tested parameters

The results of the threshold effective width from Table 3 show a difference between loading at the simple (SS) and continuous (CS) support. Consistently, lower effective widths are found at the continuous support as compared to the effective widths at the simple support. This effect can be contributed to the influence of the transverse moment.

The results from Table 3 also show a different effective width depending on the size of the loading plate. The size of the loading plate is taken into account in the French load spreading method as well as in the *fib* Model Code load spreading method.

Moreover, the results from Table 3 show that the effective width becomes smaller as the load is placed closer to the support, which corresponds to the idea of horizontal load spreading from the load towards the support at a certain angle. This parameter has an important influence on the threshold width as well as on the effective widths from the studied load spreading methods.



Since the threshold effective width is based on experimental results at failure, the effect of material non-linearity and the redistribution beyond the linear elastic material behaviour are automatically taken into account for the considered load spreading method.

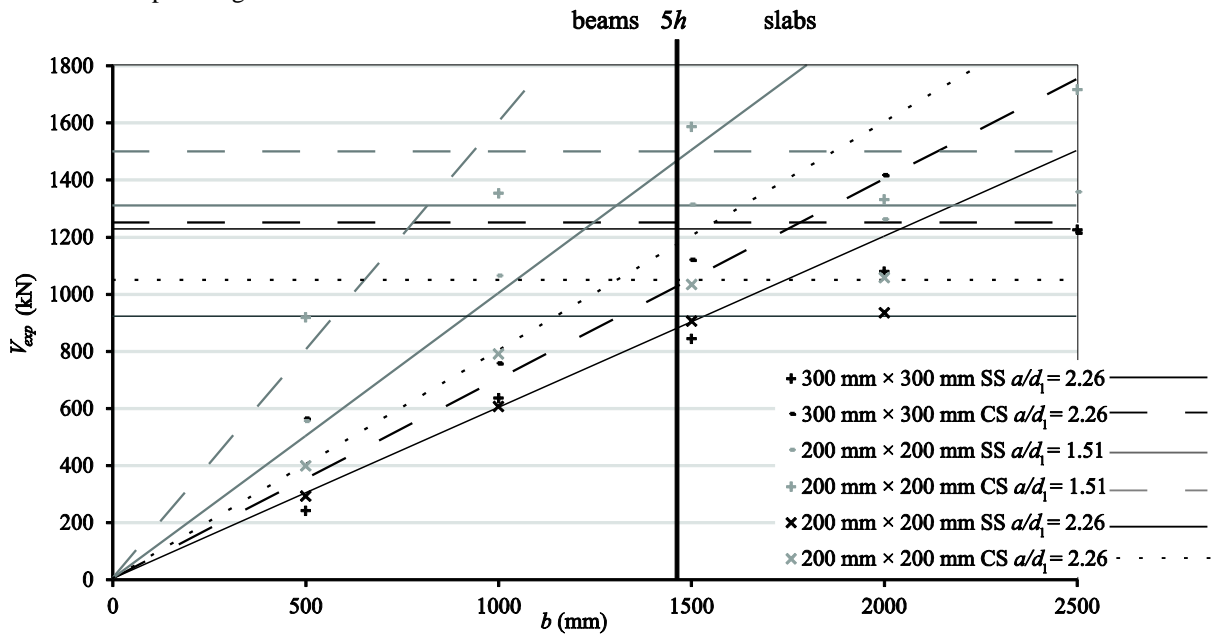


Figure 7: Influence of overall width on shear capacity. Test results for BS, BM, BL, BX, S8 and S9 are shown.

To conclude, it can be highlighted that the comparison between the threshold width and the effective widths based on the load spreading methods in Table 3 shows that the threshold width corresponds best to the effective width based on the French load spreading method. Therefore, it is recommended to take transverse load redistribution into account by using a practical load spreading method based on a  $45^\circ$  angle from the far side of the load to the face of the support.

## 6. CONSEQUENCES OF USING THE FRENCH LOAD SPREADING METHOD

As compared to load spreading methods that were used previously in the Netherlands, the French load spreading method results in a larger effective width since the load spreading in the French method is taken from the far side of the loading plate instead of from the center of the loading plate. When the effective width is larger, the resulting shear stress at the support is smaller, because the same load is distributed over a larger effective width. This result allows for more economic designs and provides a better assessment tool, as a smaller shear stress needs to be designed for when the same loads are considered.

## 7. SUMMARY AND CONCLUSIONS

In The Netherlands, shear assessment of 600 reinforced concrete solid slab bridges is necessary. These assessments are carried out following a Level of Approach approximation. The first Level of Approach is a spreadsheet-based method, the Quick Scan, which gives a first estimate of the shear capacity of a solid slab bridge. For this method, a practical way to take transverse load redistribution into account was sought. Transverse load redistribution has a beneficial effect on the shear capacity of slabs subjected to concentrated loads. A practical way to translate the principle of transverse load redistribution is by using a load spreading method. Methods from The Netherlands, France and as recommended by *fib* Model Code 2010 are studied.

To study the load spreading methods, experiments on specimens with increasing widths (from 0.5 m to 2.0 m in 0.5 increments) are carried out and compared to results of experiments on slabs of 2.5 m wide. In total, 24 experiments on 12 specimens are carried out, and combined with 4 experiments from prior testing. The specimens failed in shear and punching, often in a combination of both failure mechanisms.

The results for the shear capacity were studied as a function of the specimen width to determine the threshold width after which a further increase in the slab width does not lead to a further increase in shear capacity. The threshold widths from the series of experiments are compared to the resulting effective widths from the load spreading methods, and it is found that the French load spreading method leads to the best results. The French load spreading method (load spreading from the far side of the load to the face of the support) leads to the largest effective width of the studied methods, and thus to the lowest shear stresses. As such, this method results in a more economic design and assessment. The French load spreading method was incorporated into the first Level of Approximation for assessment, and is thus used for the shear assessment of solid slab bridges in the Netherlands.

## 8. REFERENCES

- Bažant, Z. P. and Kim, J. K. 1984. Size Effect in Shear Failure of Longitudinally Reinforced Beams, *Journal of the American Concrete Institute*, 81 (5): 456-468.
- CEN, 2003, *Eurocode 1: Actions on structures - Part 2: Traffic loads on bridges, EN 1991:2-2003*, Comité Européen de Normalisation, Brussels, Belgium, 168 pp.
- CEN, 2005, *Eurocode 2: Design of Concrete Structures - Part 1-1 General Rules and Rules for Buildings. EN 1992-1-1:2005*, Comité Européen de Normalisation, Brussels, Belgium, 229 pp.
- Code Committee 351001. 1995. *NEN 6720 Technical Foundations for Building Codes, Concrete provisions TGB 1990 - Structural requirements and calculation methods (VBC 1995)*, Civil engineering center for research and regulation, Dutch Normalization Institute, Delft, The Netherlands, 245 pp.
- Coin, A. and Thonier, H. 2007. Essais sur le cisaillement des dalles en béton armé. *Annales du bâtiment et des travaux publics*: 7-16.
- Cope, R. J. 1985. Flexural Shear Failure of Reinforced-Concrete Slab Bridges. *Proceedings of the Institution of Civil Engineers Part 2-Research and Theory*, 79 (SEP): 559-583.
- fib. 2012. *Model code 2010: final draft*, International Federation for Structural Concrete; Lausanne, 676 pp.
- Goldbeck, A. T. 1917. The influence of total width on the effective width of reinforced concrete slabs subjected to central concentrated loading. *ACI Journal Proceedings*, 13 (2): 78-88.
- Lantsoght, E., van der Veen, C., de Boer, A. and Walraven, J. 2014. Transverse Load Redistribution and Effective Shear Width in Reinforced Concrete Slabs. *Heron*: 29 pp. (in press).
- Lantsoght, E. O. L., 2011, Shear tests of reinforced concrete slabs: experimental data of undamaged slabs, *Stevinrapport nr 25.5-11-07*, Delft University of Technology, The Netherlands, 512 pp.
- Lantsoght, E. O. L., van der Veen, C. and Walraven, J. C. 2012b. Shear capacity of slabs and slab strips loaded close to the support. *ACI SP-287, Recent Development in Reinforced Concrete Slab Analysis, Design and Serviceability*: 5.1-5.18.
- Lantsoght, E. O. L., van der Veen, C., de Boer, A. and Walraven, J. C. 2013a. Recommendations for the Shear Assessment of Reinforced Concrete Slab Bridges from Experiments *Structural Engineering International*, 23 (4): 418-426.
- Lantsoght, E. O. L., van der Veen, C. and Walraven, J. C. 2013b. Shear in One-way Slabs under a Concentrated Load close to the support. *ACI Structural Journal*, 110 (2): 275-284.
- Prochazkova, Z. and Lantsoght, E. O. L., 2011, Material properties – Felt and Reinforcement For Shear test of Reinforced Concrete Slab, *Stevin Report nr. 25.5-11-11*, Delft University of Technology, 28 pp.
- Regan, P. E. and Rezai-Jorabi, H. 1988. Shear Resistance of One-Way Slabs under Concentrated Loads. *ACI Structural Journal*, 85 (2): 150-157.
- Reißen, K. and Hegger, J. 2013. Experimentelle Untersuchungen zur mitwirkenden Breite für Querkraft von einfeldrigen Fahrbahnplatten. *Beton- und Stahlbetonbau*, 108 (2): 96-103.
- Vergoossen, R., Naaktgeboren, M., 't Hart, M., De Boer, A. and Van Vugt, E. 2013. Quick Scan on Shear in Existing Slab Type Viaducts. *International IABSE Conference, Assessment, Upgrading and Refurbishment of Infrastructures*, Rotterdam, pp. 8.
- Walraven, J. C. 2010. Residual shear bearing capacity of existing bridges. *fib Bulletin 57, Shear and punching shear in RC and FRC elements; Proceedings of a workshop held on 15-16 October 2010*, Salò, Lake Garda, Italy. pp 129-138.